A Journal of the German Chemical Society
Angewandte Chemie
GDCh
International Edition
www.angewandte.org

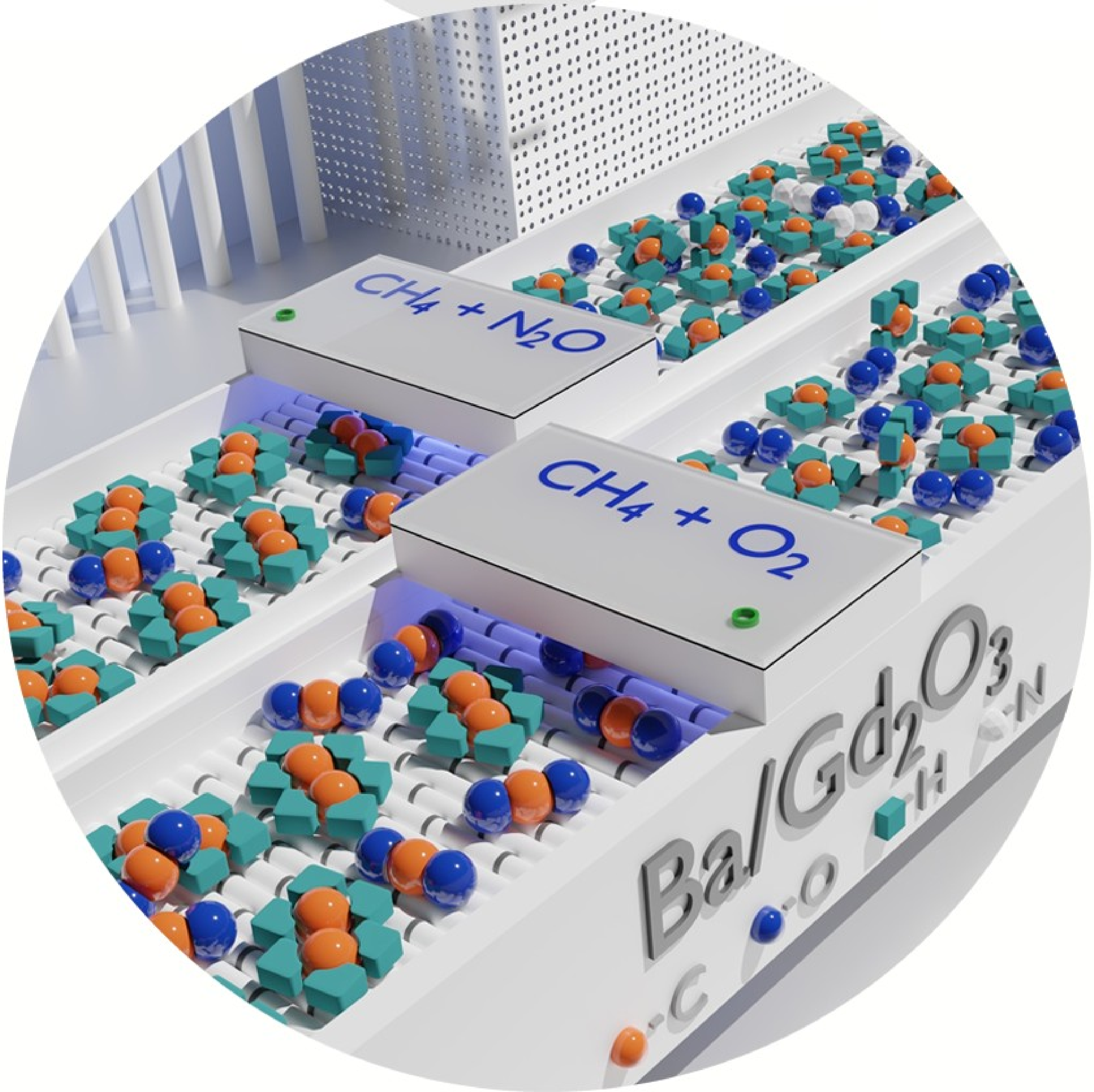

The nature of adsorbed oxygen species determines the product selectivity in the oxidative coupling of CH_4 as shown on the cover. In their Communication (e202319192), Guiyuan Jiang, Evgenii V. Kondratenko et al. describe how the formation of carbon oxides and ethane correlates with the binding strength of selective mono-atomic oxygen species. The strength affects the probability of their recombination to diatomic oxygen species oxidizing methane to carbon oxides. Cover image credit: Vita A. Kondratenko.

WILEY VCH

How to cite: Angew. Chem. Int. Ed. **2024**, e202319192
doi.org/10.1002/anie.202319192

Heterogeneous Catalysis

Fundamentals of Unanticipated Efficiency of Gd_2O_3-based Catalysts in Oxidative Coupling of Methane

Kai Wu, Anna Zanina, Vita A. Kondratenko, Lin Xu, Jianshu Li, Juan Chen, Henrik Lund, Stephan Bartling, Yuming Li, Guiyuan Jiang, and Evgenii V. Kondratenko**

Abstract: Improving the selectivity in the oxidative coupling of methane to ethane/ethylene poses a significant challenge for commercialization. The required improvements are hampered by the uncertainties associated with the reaction mechanism due to its complexity. Herein, we report about 90 % selectivity to the target products at 11 % methane conversion over Gd_2O_3-based catalysts at 700 °C using N_2O as the oxidant. Sophisticated kinetic studies have suggested the nature of adsorbed oxygen species and their binding strength as key parameters for undesired methane oxidation to carbon oxides. These descriptors can be controlled by a metal oxide promoter for Gd_2O_3.

Due to recent discoveries of natural/shale gas resources, the conversion of methane to ethane and ethylene (C_2-hydrocarbons), oxidative coupling of methane (OCM), has gained new research interest.[1] The use of O_2 as an oxidant makes this reaction more thermodynamically feasible. However, C_2-hydrocarbons are prone to oxidation to carbon oxides. Hindering these side reactions is a priority for OCM commercialization. The $Mn/Na_2WO_4/SiO_2$ system, one of the promising OCM catalysts, shows reasonable selectivity above 800 °C.[2] Catalysts based on oxides of lanthanides are also promising for OCM.[3–6] La_2O_3,[7] Sm_2O_3[8] or Nd_2O_3[9] can activate CH_4 below 700 °C but have low selectivity to the desired products.

To control product selectivity, N_2O, CO_2, or S_2 have been used instead of O_2.[10] N_2O improved C_2-hydrocarbons selectivity over various catalysts above 750 °C.[11–13] Sm_2O_3 was the only rare earth oxide tested in OCM with N_2O (N_2O–OCM), but showed low selectivity.[14] The use of N_2O is advantageous from an environmental point of view, as the global warming potential of this compound is about 300 and 10 times higher than that of CO_2 and CH_4 respectively. One disadvantage of using N_2O as oxidant is its price. N_2O is, however, formed in large quantities as a by-product in the production of adipic acid,[15] and can also be produced by the direct oxidation of NH_3,[16] which may become the basis for low-cost N_2O production in the future. Motivated by these considerations, we introduce Gd_2O_3-based materials as a promising N_2O–OCM system that is highly selective at 650–700 °C. Kinetic tests revealed how the overall pathways of the formation of C_2-hydrocarbons and carbon oxides are affected by O_2 and N_2O. Temporal analyses of products enabled us to understand the role of promoter for Gd_2O_3 and type of oxygen species in the efficient conversion of CH_4 to the target products.

Oxides of Eu, Nd, Er, La, Gd, Ho, Dy or Sm were tested in O_2-, and N_2O–OCM at 750 °C (Figure 1). The selectivity to C_{2+}-hydrocarbons (C_2–C_3 hydrocarbons) increased when O_2 was replaced by N_2O. The yield was almost unchanged over Sm_2O_3 and Dy_2O_3, decreased over Eu_2O_3 and Nd_2O_3 but increased over Ho_2O_3, La_2O_3, Er_2O_3 and Gd_2O_3 (to the highest extent). Gd_2O_3 was rarely used in OCM studies probably due to its low performance.[6,17] Ng and coworkers[17] reported about 54 % selectivity to C_{2+}-hydrocarbons at 32 % CH_4 conversion over Gd_2O_3 modified with BaO in O_2–OCM at 750 °C.

Inspired by the positive effects of Na, Sr and Ba promoters on the C_2-hydrocarbons selectivity of various catalysts,[4] we modified Gd_2O_3 accordingly. The catalysts with 10 wt % promoter (0.1NaGd, 0.1SrGd and 0.1BaGd) consisted of the cubic Gd_2O_3 phase (Figure S1a). Ba and Sr were identified as carbonates. No Na-containing phase was detected. In situ and ex situ X-ray diffraction analysis of 0.1BaGd in O_2–OCM and N_2O–OCM revealed no change in phase composition (Figures S1b,c). Pseudo in situ X-ray photoelectron spectroscopy (XPS) tests also showed no obvious effect of the reaction feed on the catalyst surface composition. There are, however, some differences in the XP spectra of Gd_2O_3 and 0.1BaGd (Figures S1d–i). The XP C 1s spectrum of 01.BaGd is characterized by a signal at about 289 eV, which can be assigned to carbonates, probably barium carbonates in agreement with XRD data. The promoter should also be responsible for the presence of a signal at about 531 eV in the XP O1s spectrum.

---

[*] K. Wu, L. Xu, J. Li, J. Chen, Dr. Y. Li, Prof. Dr. G. Jiang
State Key Laboratory of Heavy Oil Processing
China University of Petroleum
Beijing, 102249, (China)
E-mail: jianggy@cup.edu.cn

K. Wu, Dr. A. Zanina, Dr. V. A. Kondratenko, L. Xu, Dr. H. Lund, Dr. S. Bartling, Prof. Dr. E. V. Kondratenko
Department of Advanced methods for applied catalysis
Leibniz-Institut für Katalyse e.V.
Albert-Einstein-Str. 29a, 18059 Rostock (Germany)
E-mail: Evgenii.Kondratenko@catalysis.de

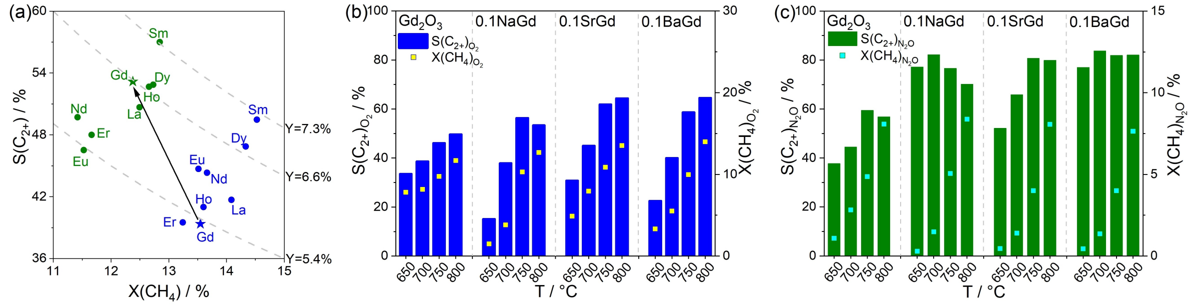

Figure 1. Results of OCM screening tests over (a) rare earth metal oxides or (b, c) Gd_2O_3-based catalysts with (a, b) O_2 (blue symbols) and (a, c) N_2O (green symbols). Reaction conditions: 40vol% CH_4, $CH_4/O_2=8$, 750 °C, $CH_4/N_2O=4$, contact time τ is (a) 0.19 and (b, c) 0.047 $g_{cat}\cdot min\cdot mmol_{CH4}{}^{-1}$.

The C_{2+}-selectivity in O_2–OCM over Gd_2O_3, 0.1NaGd, 0.1SrGd and 0.1BaGd at 650 °C is 33.6 %, 15.1 %, 30.8 %, and 22.6 %, respectively (Figure 1b, Table S1). When the temperature increased, the selectivity increased, too. Such a dependence is consistent with previous O_2–OCM studies, which concluded that high temperatures are essential to achieve high C_{2+}-selectivity.[1,2]

Compared with O_2–OCM, N_2O–OCM over 0.1BaGd reached the selectivity of 77 % at 0.44 % CH_4 conversion at 650 °C. The selectivity did not decrease even though the conversion increased to 7.5 % with increasing the reaction temperature to 800 °C (Figure 1c, Table S2). The selectivity of 0.1NaGd passed a maximum with increasing temperature while that of Gd_2O_3 and 0.1SrGd increased. Since the strongest positive effect was observed for 0.1BaGd, we further focused on this system. N_2O–OCM tests with $BaCO_3$ and BaO at 650 °C showed poor performance of these materials (Figure S2), so, Ba must be a promoter for Gd_2O_3. To understand the role of this promoter, BaGd catalysts with different Ba loading were further prepared and tested in O_2–OCM and N_2O–OCM.

In O_2–OCM at 700 °C, the rate of overall CH_4 consumption (r(CH_4)) as well as the rates of CH_4 conversion to C_2H_6 (r(C_2H_6)), C_2H_4 (r(C_2H_4)), CO_2 (r(CO_2)) and CO (r(CO)) decreased linearly with Ba loading (Figure 2a–c, Figure S3). Contrarily, an unexpected effect of Ba loading on these rates was observed in N_2O–OCM. Although Ba addition reduced r(CH_4) (Figure 2a), r(C_2H_6) followed a volcano-type dependence on the Ba/Gd ratio (Figure 2b). The r(C_2H_6) of all *x*BaGd was higher than that of Gd_2O_3. The r(C_2)/r(CO_x) ratio of *x*BaGd in O_2–OCM is close to 1, but is significantly higher in N_2O–OCM, reaching its highest value of about 9 for 0.1BaGd (Figure 2d). Increasing the Ba loading further has, however, a negative effect. Importantly,

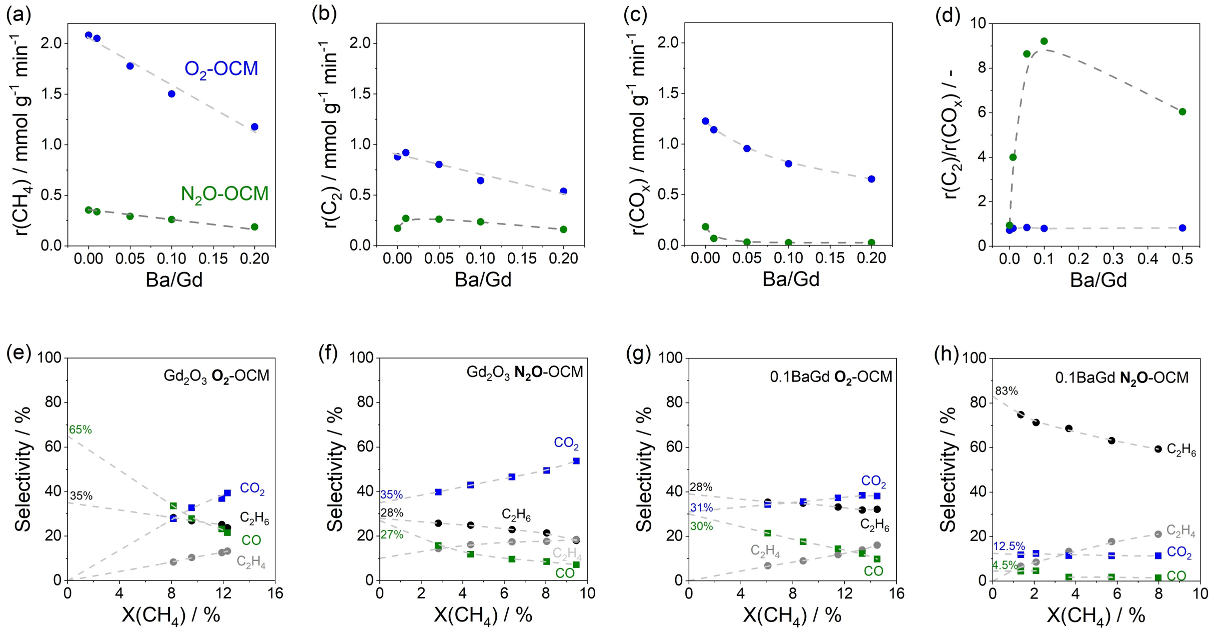

Figure 2. Effects of Ba loading on (a) r(CH_4), (b) r(C_2), and (c) r(CO_x). (d) The ratio of r(C_2)/r(CO_x) versus Ba/Gd in O_2- or N_2O–OCM. (e–h) Primary selectivity in O_2- or N_2O–OCM over Gd_2O_3 and 0.1BaGd. Reaction conditions: 40vol% CH_4, $CH_4/O_2=8$, $CH_4/N_2O=4$, 700 °C, τ is 0.037 $g_{cat}\cdot min\cdot mmol_{CH4}{}^{-1}$ (O_2–OCM) or 0.093 $g_{cat}\cdot min\cdot mmol_{CH4}{}^{-1}$ (N_2O–OCM).

r(CO_2) and r(CO) decrease with Ba loading stronger in N_2O–OCM than in O_2–OCM (Figure S4).

The effects of O_2 and N_2O on the reaction pathways to CO, CO_2, C_2H_4, and C_2H_6 were elucidated by analyzing the selectivity-conversion relationships obtained through varying the space velocity at 700 °C (Figure 2). To distinguish between primary (formed from CH_4) and secondary (not formed from CH_4) products, the selectivity to each product was extrapolated to zero CH_4 conversion. The products with non-zero selectivity should be formed directly from CH_4, while those with a zero value are secondary products derived from primary products. Regardless of the oxidant, CO and C_2H_6 are primarily products formed over 0.1BaGd or Gd_2O_3 (Figure 2e–h). This is also true for CO_2 formation in N_2O- and O_2–OCM over 0.1BaGd and in N_2O–OCM over Gd_2O_3.

Replacing O_2 with N_2O decreased the primary selectivity to C_2H_6 and CO over Gd_2O_3 from 35 to 28 % and from 65 to 27 %, respectively, but increased the primary selectivity to CO_2 from 0 to 35 % (Figure 2e,f). Conversely, the primary selectivity to C_2H_6 over 0.1BaGd increased from 39 to 83 % (Figure 2g,h). This increase was accompanied by a decrease in the primary selectivity to CO and CO_2 from 30 to 4.5 % and from 31 to 12.5 %, respectively. Thus, the modification of Gd_2O_3 with Ba is pivotal for improving the efficiency of CH_4 conversion to C_2H_6 in the presence of N_2O.

In both O_2- and N_2O–OCM, primarily formed C_2H_6 is converted to C_2H_4 as reflected by the decreasing and increasing dependence of the selectivity to these products on CH_4 conversion (Figure 2). N_2O appears to be superior to O_2 in promoting this reaction as indicated by the higher selectivity ratio of C_2H_4 to C_2H_6 (Figure S5). The selectivity to CO and CO_2 decreased and increased respectively with increasing methane conversion due to oxidation of CO to CO_2. Since the selectivity to C_{2+}-hydrocarbons or carbon oxides does not change significantly with increasing CH_4 conversion, the desired products are not involved in consecutive oxidation reactions (Figure S6).

Direct N_2O decomposition over Gd_2O_3 and 0.1BaGd was also investigated. Consistent with proposed mechanisms for this reaction over various catalysts,[18] N_2O first reacts with an anion vacancy ([ ]) to form gas-phase N_2 and a monatomic adsorbed oxygen species ([O]) (eq 1). Gas-phase O_2 can be formed by a reversible recombination of two [O] (eq 2) or an irreversible reaction of N_2O with [O] (eq 3).

To distinguish between these mechanisms, we investigated whether the rate of N_2O decomposition is affected by the addition of O_2. A negative effect was observed (Figure S7). Thus, O_2 should be formed according to eq 2. The difference between the catalysts in the inhibiting O_2 effect is related to the kinetics of O_2 formation/desorption, the latter processes being slower on the modified catalyst compared to Gd_2O_3.

$$N_2O + [] \rightarrow N_2 + [O] \qquad (1)$$

$$[O] + [O] \rightleftarrows \ldots \rightleftarrows O_2 + 2[] \qquad (2)$$

$$N_2O + [O] \rightarrow N_2 + O_2 + [] \qquad (3)$$

The dissimilar ability of Gd_2O_3 and its modified counterparts to form O_2 from N_2O was independently proved by analyzing the height-normalized responses of O_2 and N_2 (Figure 3a,b and Figure S8) recorded after pulsing of

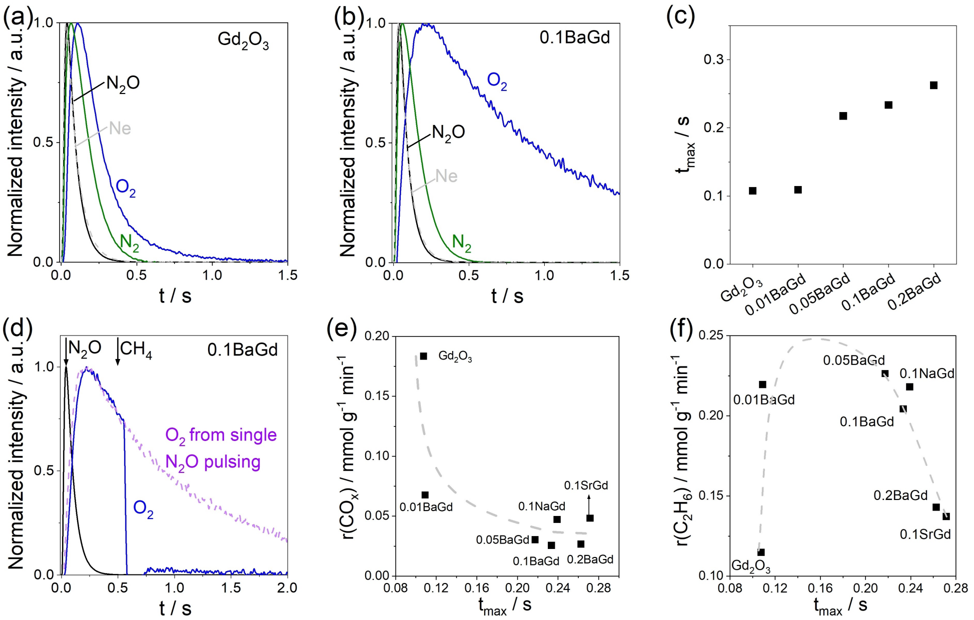

Figure 3. The height-normalized responses of N_2O, N_2 and O_2 after pulsing N_2O over (a) Gd_2O_3 and (b) 0.1BaGd. (c) The time of maximum intensity (t_{max}) of the height-normalized response of O_2 after pulsing N_2O over *x*BaGd. (d) The height-normalized responses of N_2O and O_2 after N_2O–CH_4 pump-probe tests with a time delay of 0.5 s over 0.1BaGd. (e) r(CO_x) in N_2O–OCM versus t_{max} of O_2. (f) r(C_2H_6) in N_2O–OCM versus t_{max} of O_2.

N_2O:Ne = 1 at 700 °C in a temporal analysis of products reactor.[19] Since the O_2 concentration is still high when the N_2 concentration is zero, recombination of [O] originated from N_2O should contribute to O_2 formation.

For a simple qualitative analysis of the rates of O_2 and N_2 formation, we use the time of maximum intensity (t_{max}) of the height-normalized O_2 and N_2 responses. For both unmodified and modified Gd_2O_3, O_2 formation should limit N_2O decomposition because t_{max} of O_2 is significantly higher than t_{max} of N_2 (Table S3). As the former value becomes larger in the presence of Ba promoter and with its rising concentration, the rate of [O] recombination should be hindered by the promoter probably due to an increase in the bonding strength of [O]. This statement is supported by the time required to reach zero O_2 concentration (Figure S9).

The involvement of [O] in CH_4 activation was verified by pump-probe experiments with N_2O and CH_4. When these gases were pulsed with a time delay (Δt) of 0.5 s, the t_{max} value of the O_2 response did not change compared to that of single N_2O pulses (Figures 3d and S10a). Its intensity, however, decreased sharply when CH_4 entered the reactor because [O] oxidized this alkane to carbon oxides. C_2H_6 was not observed due to the high-vacuum conditions, which are unfavorable for recombination of methyl radicals. An increase in Δt caused a decrease in coverage by [O] due to recombination of these species to O_2 (eq.2), which is detrimental to methane conversion (Figure S10b). The lower conversion of CH_4 over Gd_2O_3 compared to 0.1BaGd is explained by the higher recombination rate of [O] to gas-phase O_2. Lattice oxygen of Gd_2O_3 or BaO is significantly less active for CH_4 oxidation than [O] as proven by pulse experiments with CH_4 only (Figure S10c–f).

Based on the above results, we propose that the different activity of Gd_2O_3 and its modified counterparts to form O_2 from N_2O is the origin of the dissimilar behavior of these catalysts in O_2- and N_2O–OCM. Since the recombination of [O] to gas-phase O_2 over the modified catalysts (eq 2) is slow, CH_4 should react mainly with [O] in N_2O–OCM. The much faster recombination of [O] over Gd_2O_3 favors the formation of gas-phase O_2. Thus, O_2–OCM could occur during N_2O–OCM over Gd_2O_3. This scenario can explain why in contrast to Gd_2O_3 the selectivity to C_{2+}-hydrocarbons is improved over *x*BaGd, 0.1NaGd and 0.1SrGd when O_2 is replaced by N_2O (Figures 1 and 2g,h). This explanation is indirectly supported by a negative relationship between t_{max} of the O_2 response in N_2O pulse tests and r(CO_x) or r(CH_4) in N_2O–OCM (Figures 3e, S11a). The stronger the oxygen species are bound, the lower their ability to oxidize CH_4/C_2-hydrocarbons to carbon oxides. The volcano-type relationship between r(C_2H_6) and Ba loading in Figure 2b can now be rationalized. This rate also follows a volcano-type relationship with t_{max} (Figure 3f). Importantly, 0.1NaGd and 0.1SrGd fit this relationship. Thus, an appropriate binding strength of [O] to the catalyst surface is vital to achieve the maximum r(C_2H_6), while the r(CH_4) decreases with the strength due to the inhibition of CO_x formation (Figure S11b).

The impact of the performance of 0.1BaGd achieved in N_2O–OCM is demonstrated by Figure 4a, where data from previous N_2O–OCM studies with different catalysts are also

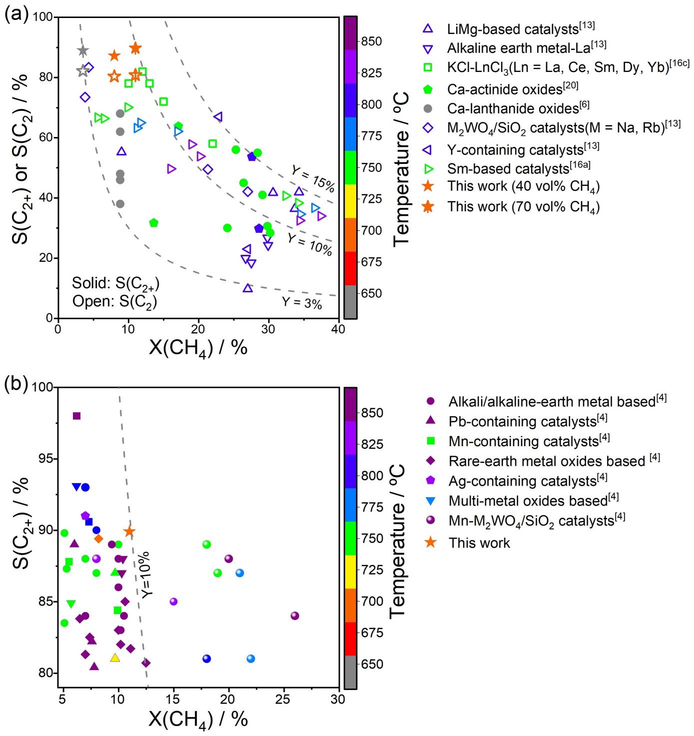

Figure 4. Selectivity-conversion values for C_2- or C_{2+}-hydrocarbons obtained in the present and previous (a) N_2O–OCM or (b) O_2–OCM studies. Current reaction conditions: τ is 0.75 or 0.43 $g_{cat}\cdot min\cdot mmol_{CH_4}^{-1}$, $CH_4/N_2O = 4$. Literature data are given in Tables S4 for (a) and S5 for (b).

presented (Table S4). The 0.1BaGd catalyst showed the selectivity to C_{2+} and C_2-hydrocarbons of 89 % and 82 % at 3.5 % CH_4 conversion, and 87 % and 80 % at 8 % CH_4 conversion at 650 and 700 °C, respectively. Performing N_2O–OCM with a feed containing 70 vol % CH_4 further improved the selectivity to 89.8 % and 81 % at 11 % CH_4 conversion. All catalysts tested so far were less efficient. Potassium lanthanide chlorides,[16c] Ca-actinide oxides,[20] Ca-lanthanide oxides,[6] Sm-based catalysts,[16a] LiMg-based catalysts,[13] and Na_2WO_4-based catalysts[13] operated at higher temperatures and achieved similar C_{2+}-hydrocarbon yields but lower selectivity. According to a techno-economic analysis,[21] however, the final price of ethylene is more influenced by selectivity than by methane conversion.

The C_{2+}-selectivity of 90% at 11% CH_4 conversion obtained in the present study in N_2O–OCM at 700 °C is also remarkable in view of the O_2–OCM data obtained over different catalysts summarized in the database of Ref.,[4] which contains about 1800 selectivity-conversion data points. Using this database, we have selected catalysts showing the selectivity to C_2-hydrocarbons above 80% at CH_4 conversion degrees above 5% (Table S5). Only the most promising Mn/Na_2WO_4/SiO_2 catalysts achieved the selectivity between 81 and 89 % at methane conversion above 15 % but above 750 °C (Figure 4b).

In conclusion, we have unveiled Gd_2O_3 modified with Ba, Na or Sr as a highly efficient system for N_2O–OCM at 650–700 °C. The promoter enhances the binding strength of mono-atomically adsorbed oxygen species formed from N_2O, which is pivotal for hindering their recombination to a diatomic adsorbed oxygen species, which shows higher ability for the direct CH_4 oxidation to carbon oxides. The mono-atomic species appears to have a higher selectivity for the conversion of CH_4 to C_2H_6. The established fundamentals provide clarity on the role of oxygen species in controlling product selectivity and can contribute to the design of OCM catalysts that also operate selectively with O_2.

Acknowledgements

This work is supported by the National Natural Science Foundation of China (Grant Nos. 21961132026, 22225807, 22021004) and Deutsche Forschungsgemeinschaft (KO 2261/11-1) within a joint Sino-German research project. The authors thank Kathleen Schubert for ex situ XRD measurements. Kai Wu acknowledges the support from the China Scholarship Council. Open Access funding enabled and organized by Projekt DEAL.

Conflict of Interest

The authors declare no conflict of interest.

Data Availability Statement

The data that support the findings of this study are available from the corresponding author upon reasonable request.

Keywords: oxidative coupling of methane · N_2O–OCM · temporal analysis of products · reaction mechanism · oxygen species

---

[1] a) E. V. Kondratenko, T. Peppel, D. Seeburg, V. A. Kondratenko, N. Kalevaru, A. Martin, S. Wohlrab, *Catal. Sci. Technol.* **2017**, *7*, 366–381; b) P. Schwach, X. Pan, X. Bao, *Chem. Rev.* **2017**, *117*, 8497–8520.

[2] a) P. Wang, G. Zhao, Y. Wang, Y. Lu, *Sci. Adv.* **2017**, *3*, e1603180; b) S. Arndt, T. Otremba, U. Simon, M. Yildiz, H. Schubert, R. Schomäcker, *Appl. Catal. A* **2012**, *425–426*, 53–61; c) D. Kiani, S. Sourav, J. Baltrusaitis, I. E. Wachs, *ACS Catal.* **2019**, *9*, 5912–5928.

[3] H. Wang, R. Schmack, S. Sokolov, E. V. Kondratenko, A. Mazheika, R. Kraehnert, *ACS Catal.* **2022**, *12*, 9325–9338.

[4] U. Zavyalova, M. Holena, R. Schlögl, M. Baerns, *ChemCatChem* **2011**, *3*, 1935–1947.

[5] A. Dedov, A. Loktev, I. Moiseev, A. Aboukais, J.-F. Lamonier, I. Filimonov, *Appl. Catal. A* **2003**, *245*, 209–220.

[6] A. C. Ferreira, T. A. Gasche, J. Leal, J. B. Branco, *J. Mol. Catal.* **2017**, *443*, 155–164.

[7] Q. Zhou, Z.-Q. Wang, Z. Li, J. Wang, M. Xu, S. Zou, J. Yang, Y. Pan, X.-Q. Gong, L. Xiao, *ACS Catal.* **2021**, *11*, 14651–14659.

[8] A. S. Jones, D. Aziz, J. Ilsemann, M. Bäumer, H. Hagelin-Weaver, *Catal. Today* **2021**, *365*, 58–70.

[9] F. Alahmadi, A. Bavykina, D. Poloneeva, A. Ramirez, R. Schucker, J. Gascon, *AlChE J.* **2023**, *69*, e17959.

[10] A. M. Arinaga, M. C. Ziegelski, T. J. Marks, *Angew. Chem. Int. Ed.* **2021**, *60*, 10502–10515.

[11] K. Langfeld, B. Frank, V. E. Strempel, C. Berger-Karin, G. Weinberg, E. V. Kondratenko, R. Schomäcker, *Appl. Catal. A* **2012**, *417*, 145–152.

[12] Z. Aydin, A. Zanina, V. A. Kondratenko, J. Rabeah, J. Li, J. Chen, Y. Li, G. Jiang, H. Lund, S. Bartling, *ACS Catal.* **2022**, *12*, 1298–1309.

[13] H. Liu, Y. Wei, J. Caro, H. Wang, *ChemCatChem* **2010**, *2*, 1539–1542.

[14] a) H. Özdemir, M. F. Öksüzömer, M. Ali Gürkaynak, *Chem. Eng. Commun.* **2019**, *206*, 48–60; b) O. Buyevskaya, M. Baems, *Catal. Today* **1994**, *21*, 301–308; c) J. B. Branco, A. C. Ferreira, A. M. B. do Rego, A. M. Ferraria, G. Lopes, T. A. Gasche, *J. Mol. Liq.* **2014**, *191*, 100–106.

[15] a) A. Shimizu, K. Tanaka, M. Fujimori, *Chemosphere-Global Change Science* **2000**, *2*, 425–434; b) J. Rios, J. Lebeau, T. Yang, S. Li, M. D. Lynch, *Green Chem.* **2021**, *23*, 3172–3190.

[16] a) V. Parmon, G. Panov, A. Uriarte, A. Noskov, *Catal. Today* **2005**, *100*, 115–131; b) J. Ludvíková, M. Jabłońska, K. Jirátová, L. Chmielarz, J. Balabánová, F. Kovanda, L. Obalová, *Res. Chem. Intermed.* **2016**, *42*, 2669–2690; c) Z. Tang, I. Surin, A. Rasmussen, F. Krumeich, E. V. Kondratenko, V. A. Kondratenko, J. Pérez-Ramírez, *Angew. Chem. Int. Ed.* **2022**, *61*, e202200772.

[17] C. Au, K. Chen, C. Ng, *Appl. Catal. A* **1998**, *170*, 81–92.

[18] a) E. V. Kondratenko, V. A. Kondratenko, M. Santiago, J. Pérez-Ramírez, *Appl. Catal. B* **2010**, *99*, 66–73; b) A. Anshits, E. Kondratenko, N. Maksimov, *Catal. Today* **1994**, *21*, 281–287.

[19] a) J. T. Gleaves, G. S. Yablonskii, P. Phanawadee, Y. Schuurman, *Appl. Catal. A* **1997**, *160*, 55–88; b) J. Pérez-Ramírez,

E. V. Kondratenko, *Catal. Today* **2007**, *121*, 160–169; c) K. Morgan, N. Maguire, R. Fushimi, J. Gleaves, A. Goguet, M. Harold, E. V. Kondratenko, U. Menon, Y. Schuurman, G. Yablonsky, *Catal. Sci. Technol.* **2017**, *7*, 2416–2439.

[20] J. B. Branco, A. C. Ferreira, J. P. Leal, *J. Mol. Catal. A* **2014**, *390*, 45–51.

[21] A. Cruellas, J. Bakker, M. van Sint Annaland, J. Medrano, F. Gallucci, *Energy Convers. Manage.* **2019**, *198*, 111789.

[22] A. Perechodjuk, V. A. Kondratenko, H. Lund, N. Rockstroh, E. V. Kondratenko, *Chem. Commun.* **2020**, *56*, 13021–13024.

Manuscript received: December 12, 2023
Accepted manuscript online: January 25, 2024
Version of record online: ■■, ■■

Communications

Heterogeneous Catalysis

K. Wu, A. Zanina, V. A. Kondratenko, L. Xu,
J. Li, J. Chen, H. Lund, S. Bartling, Y. Li,
G. Jiang,*
E. V. Kondratenko* ________ **e202319192**

Fundamentals of Unanticipated Efficiency of Gd_2O_3-based Catalysts in Oxidative Coupling of Methane

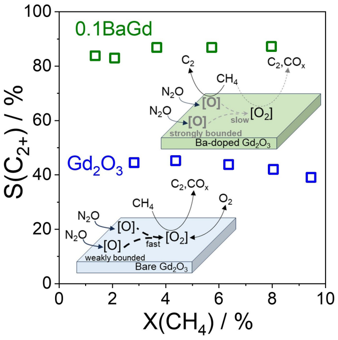

Kinetic tests combined with temporal analysis of products revealed the fundamentals relevant for regulating the efficiency of the oxidative coupling of CH_4 to C_2H_6 over Gd-based catalysts. When Gd_2O_3 is modified with Na, Sr or Ba, the use of N_2O instead of O_2 significantly improves the selectivity even at 650 °C. The promoters affect the binding strength of monoatomic oxygen species derived from N_2O and thus control the methane oxidation to carbon oxides.